Biologically Important Conformations of Aminoglycoside Antibiotics Bound to an Aminoglycoside 3′-Phosphotransferase as Determined by Transferred Nuclear Overhauser Effect Spectroscopy†

James R. Cox and Engin H. Serpersu*

Department of Biochemistry, University of Tennessee, Knoxville, Tennessee 37996-0840

Received October 25, 1996; Revised Manuscript Received December 24, 1996⊗

ABSTRACT: NMR spectroscopy has been used to study the interaction of aminoglycoside antibiotics with an aminoglycoside antibiotic 3′-phosphotransferase [APH(3′)-IIIa]. APH(3′)-IIIa is an enterococcal enzyme that is responsible for the ATP-dependent *O*-phosphorylation of a broad range of aminoglycoside antibiotics. The NMR method of transferred nuclear Overhauser effect spectroscopy (TRNOESY) was used to detect intra- and inter-ring NOEs for butirosin A and amikacin in their respective ternary complexes with APH(3′)-IIIa and ATP. NOE-derived distance constraints were used in energy minimization and dynamics routines to yield enzyme-bound structures for butirosin A. These structures suggest that the 2,6-diamino-2,6-dideoxy-D-glucose and D-xylose rings have restricted motions and are in a stacking arrangement. The TRNOE spectra for amikacin suggest that the 6-amino-6-deoxy-D-glucose ring is flexible when the antibiotic is bound to APH(3′)-IIIa. The ^{15}N resonances of butirosin A were assigned and the pK_a values of the amino groups of butirosin A and amikacin were determined by ^{15}N NMR spectroscopy. The N3 amino groups of butirosin A and amikacin have lowered pK_a values, which is attributed to the (*S*)-4-amino-2-hydroxybutyryl (AHB) group of the antibiotics. This work provides an insight into the geometrical and electrostatic nature of aminoglycoside antibiotics bound to a modifying enzyme and will provide a basis for the design of inhibitors of APH(3′)-IIIa.

Aminoglycoside antibiotics are a class of aminocyclitol antibiotics and were one of the first antibacterial agents to be clinically useful (Schatz *et al*., 1944). These antibiotics bind to the bacterial 30S ribosomal subunit and interfere with normal protein biosynthesis, which eventually leads to cell death (Davies, 1987). Aminoglycosides were once used extensively to treat infections caused by enterococci and staphylococci; however, these bacteria have responded by producing an array of enzymes which covalently modify the antibiotics, thereby rendering them inoffensive (Davies, 1994; Shaw *et al*., 1993). These modifying enzymes can be classified as *O*-phosphotransferases (APH),[1] *O*-nucleotidyltransferases, and *N*-acetyltransferases (Umezawa & Kondo, 1982). The 3′-phosphotransferases are widely distributed in pathogenic bacteria, and at least seven different isozymes have been identified (Shaw *et al*., 1993).

One particular enterococcal 3′-phosphotransferase, APH(3′)-IIIa, has the broadest substrate specificity of all the isozymes (Shaw *et al*., 1993). Recently, this enzyme has been overexpressed and characterized as an ATP-dependent aminoglycoside kinase (McKay *et al*., 1994). APH(3′)-IIIa regiospecifically phosphorylates 4,6-disubstituted aminoglycosides such as kanamycin and amikacin at the 3′-OH group of the 6-amino-6-deoxy-D-glucose ring. Lividomycin A, a 4,5-disubstituted aminoglycoside, does not have a 3′-OH group but can be phosphorylated at the 5″-OH group of the ribose ring. Other 4,5-disubstituted aminoglycosides, such as butirosin A and neomycin B, can be phosphorylated at both the 3′- and 5″-hydroxyl groups (Thompson *et al*., 1996a). The initial phosphotransfer is favored at the 3′-OH group of butirosin A and at the 5″-OH group of neomycin B.

A wealth of kinetic evidence based on product and dead-end inhibition (McKay & Wright, 1995), along with viscosity and solvent isotope effects (McKay & Wright, 1996), support a Theorell−Chance mechanism for APH(3′)-IIIa. Additionally, positional isotope experiments were consistent with a direct attack of the reactive hydroxyl group of the aminoglycoside on the γ-phosphate of ATP (Thompson *et al*., 1996b). Therefore, the mechanism of APH(3′)-IIIa involves the initial binding of ATP, a fast step involving the association of the aminoglycoside and the dissociation of phosphorylated product, followed by the slow release of ADP.

We have used transferred nuclear Overhauser effect spectroscopy and molecular modeling in order to further investigate the conformational nature and dynamics of APH(3′)-IIIa-bound aminoglycoside antibiotics. Amikacin and butirosin A (Figure 1) were used in this study because their arrangements at the active site of APH(3′)-IIIa have been previously determined (Cox *et al*., 1996). A greater knowledge of the geometry of these aminoglycosides at the active

† This research was funded through a grant from the NIH (E.H.S., GM-42661). This study made use of the National Magnetic Resonance Facility at Madison, which is supported by NIH Grant RR02301 from the Biomedical Research Technology Program, National Center for Research Resources. Equipment in the facility was purchased with funds from the University of Wisconsin, the NSF Biological Instrumentation Program (Grant DMB-8415048), the NIH Biomedical Research Technology Program (Grant RR02301), the NIH Shared Instrumentation Program (Grant RR02781), and the U.S. Department of Agriculture.

* To whom correspondence should be addressed. Phone: 423-974-2668. Fax: 423-974-6306. E-mail: Serpersu@bionmr.bio.utk.edu.

⊗ Abstract published in *Advance ACS Abstracts,* February 1, 1997.

[1] Abbreviations: APH, aminoglycoside phosphotransferase; COSY, correlated spectroscopy; HSQC, heteronuclear single-quantum coherence; TRNOESY, transferred nuclear Overhauser spectroscopy; Me, metal.

S0006-2960(96)02682-7 CCC: $14.00

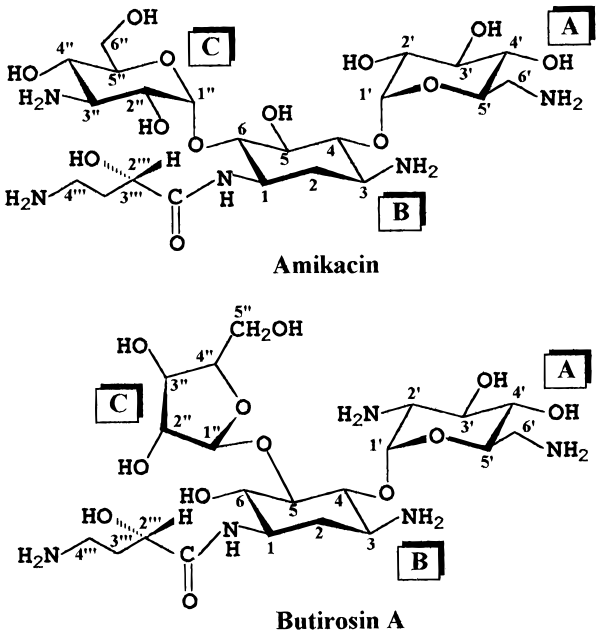

FIGURE 1: Structures of amikacin and butirosin A. In each antibiotic, the primed ring is labeled with an A and the double-primed ring with a C, and the 2-deoxystreptamine ring is denoted with a B.

site of the enzyme will serve to explain their regiochemistry and catalytic efficiency of phosphorylation. The proton resonances of amikacin (Anderson *et al*., 1988; Thompson *et al*., 1996a) and butirosin A (Cox & Serpersu, 1995) have been previously reported. In butirosin A, the primed ring is 2,6-diamino-2,6-dideoxy-D-glucose (ring A) and the double-primed ring is D-xylose (ring C). In amikacin, the primed ring is 6-amino-6-deoxy-D-glucose (ring A) and the unprimed ring is 3-amino-3-deoxy-D-glucose (ring C). The unprimed ring (ring B) in amikacin and butirosin A is 2-deoxystreptamine, modified at N1 with a (*S*)-4-amino-2-hydroxybutyryl group (AHB), which is denoted with a triple prime.

Since aminoglycoside antibiotics are highly polar and have a chance to be highly positively charged, the driving force for complexation between APH(3′)-IIIa and aminoglycosides may be electrostatic. Electrostatic interactions in neamine and kanamycin A phosphorylation have recently been demonstrated with 3′-phosphotransferases, type Ia and IIa (Roestamadji *et al*., 1995), and suggested in APH(3′)-IIIa (McKay *et al*., 1996). Therefore, we have used ^{15}N NMR spectroscopy to determine the pK_a values of the amino groups of amikacin and butirosin A.

The ultimate goal in studying the interactions of aminoglycoside antibiotics with phosphorylating enzymes is to provide a basis for a rational drug design to produce enzyme inhibitors. Gaining a knowledge of the geometrical and electrostatic attributes of enzyme-bound substrates is essential in the design of non-aminoglycoside inhibitors, which may be the key to recapturing the effectiveness of aminoglycoside antibiotics.

MATERIALS AND METHODS

Chemicals. Amikacin, butirosin A (sulfate salt), and ATP were from Sigma. Additional butirosin A was a gift from D. Baker, Department of Chemistry, University of Tennessee. D_2O and deuterated Tris (Tris-d_{11}) were from Isotec, and deuterium chloride and sodium deuteroxide were from MSD Isotopes. APH(3′)-IIIa was provided by G. Wright, McMaster University, Hamilton, Ontario, Canada, and also purified in this laboratory as described previously (McKay *et al*., 1994).

TRNOESY Experiments. APH(3′)-IIIa was first dialyzed against 2 mM Tris-d_{11} buffer (pH 6.8) in order to avoid the interference of Tris protons. The enzyme was then exchanged into D_2O by three cycles of lyophilization and redissolving in D_2O. The aminoglycosides and ATP were dissolved directly into D_2O, underwent two cycles of lyophilization, and were redissolved in D_2O. Samples contained 0.20 mM APH(3′)-IIIa, 5 mM amikacin or butirosin A, 5 mM ATP, 5 mM $CaCl_2$, and 20 mM Tris-d_{11} buffer (pH 6.8). The NOESY spectra were collected in the phase-sensitive mode with the transmitter offset placed on the HDO resonance, which was irradiated with low power during a relaxation delay of 1.8 s to suppress the H_2O signal. A total of 256 FIDs of 2k were collected. Mixing times of 40, 80, 120, and 160 ms were employed, and the data were zero-filled to 1k points in t_1 and were multiplied by a shifted sine^2 window function before Fourier transformation.

Distance Calculations. The volume of the NOE cross-peaks in the TRNOESY experiment (80 ms) was calculated in the FELIX 95 software package (BIOSYM/Molecular Simulations) operating on a Silicon Graphics Indigo-2 workstation. The volume of the cross-peak between H1′ and H2′ was taken to represent a calibration distance of 2.38 Å. The remaining NOE volumes were converted into distance constraints by using measured cross-peak volumes, which are proportional to the sixth power of the distance between proton pairs (Gronenborn & Clore, 1985; Scheffler *et al*., 1995; Casset *et al*., 1996). A generous error of ±40% was employed for the NOE cross-peak volumes used to calculate the distance constraints.

This takes into account the slight variation in T_1 values (0.6−0.9 s) observed for the protons of butirosin A when bound to the enzyme. %NOE values were calculated by dividing the volume of a cross-peak by the volume of the H3‴−H3‴ cross-peak at each mixing time and multiplying by 100. Similar distance calculations were obtained when the 40 ms TRNOE spectrum was analyzed.

Molecular Dynamics and Minimization. The aminoglycosides were created with Insight II (1995 version) (BIOSYM/Molecular Simulations) operating on a Silicon Graphics Indigo-2 workstation. All calculations were accomplished with the AMBER force field (Weiner *et al*., 1986) interfaced with the molecular mechanics package DISCOVER (BIOSYM/Molecular Simulations) on the same workstation. All potential types and charges of the aminoglycosides were set according to Homans's potential types for carbohydrates in the AMBER force field (Homans, 1990). The amino groups of the antibiotics were protonated, and the nitrogens of these groups were given a formal charge of +1.00, on the basis of the determined pK_a values (see below).

To generate random structures of the aminoglycosides, they were subjected to unrestrained molecular dynamics at 600 K for 1000 ps. Distance constraints, derived from the TRNOE studies, were applied to the random structures and underwent constrained molecular dynamics (500 ps) followed by conjugate gradient minimization (100 iterations) at 400, 350, and finally 300 K. As the final step, the structures underwent steepest descents minimization until the rms derivative was less than 0.001 kcal/Å. All calculations were

carried out *in vacuo* with a dielectric constant of 4.00, and all force constants for the distance constraints were 50 kcal/mol Å^{-1}. The *pro-R* and *pro-S* protons of C5″ have the same chemical shift at the pH in which the TRNOESY experiments were carried out. The distance restraints reported that involved H5″ were assigned to the *pro-S* hydrogen. Similar structures were obtained when the constraints were applied to the *pro-R* hydrogen.

^{15}N and ^{1}H NMR Spectroscopy of Aminoglycosides. Amikacin (free base) was dissolved directly in 85:15 (v:v) H_2O/D_2O to a concentration of 0.8 M. Butirosin A (disulfate salt) and $Ba(OH)_2$ were dissolved in 85:15 (v:v) H_2O/D_2O to concentrations of 0.5 M. $BaSO_4$ was removed by centrifugation for 10 min at 5000*g*. ^{1}H-decoupled one-dimensional ^{15}N NMR spectra were recorded as a function of pH for butirosin A and amikacin at 40.54 MHz on a Bruker AMX-400 wide bore spectrometer at 27 °C using a 5 mm inverse broad band probe. Acquisition parameters included a spectral width of 8196.7 Hz, a 90° pulse width of 17 μs, and an acquisition time of 0.5 s. A total of 32k data points of 2000−8000 FIDs were collected. Before Fourier transformation, 10 Hz line broadening was applied. All ^{15}N chemical shifts are referenced to $^{15}NH_4Cl$. The $^{15}NH_4Cl$ (5% enriched) solution was 1 M and prepared in 85:15 (v:v) H_2O/D_2O. The pK_a values of the amino groups of amikacin and butirosin A were determined by fitting the data to a modified Hill equation (Markley, 1975) using the program P-Fit (Biosoft).

The ^{15}N assignments of butirosin A at pH 1.0 were made through the use of two-dimensional ^{1}H−^{1}H COSY and ^{1}H−^{15}N HSQC experiments. The butirosin A sample described above (adjusted to pH 1.0) was used in the two-dimensional experiments. The COSY data set was collected in the phase-sensitive mode using the time-proportional phase increment method (Marion & Wütrich, 1983). The transmitter offset was placed on the HDO resonance, which was irradiated with a low-power pulse during a relaxation delay of 1.8 s to suppress the water signal. A total of 256 FIDs of 2k were collected with a total of 32 scans per FID with a spectral width of 3205 Hz. The data were zero filled to 1k points in t_1 and multiplied by the sine window function in both dimensions before Fourier transformation. A ^{1}H−^{15}N HSQC experiment was performed at the National NMR Facility at Madison, WI (NMRFAM), on a Bruker 500 MHz spectrometer. Sixteen transients of 1k data points, with 32 increments, were collected over a spectral width of 8333 and 333 Hz in t_2 and t_1, respectively. Before Fourier transformation, the data were multiplied with a shifted sine^2 and sine window functions in t_2 and t_1, respectively.

RESULTS

TRNOESY Spectra of Butirosin A. Complete NOE buildup curves were obtained for butirosin A by recording the TRNOESY spectra at different mixing times (Figure 2). The intensities of the NOEs and the shape of the buildup curves suggest that spin diffusion is not significant at shorter mixing times. Therefore, a mixing time of 80 ms was chosen for data analysis because all of the NOEs were well developed, and this mixing time is in the linear part of the buildup curve for all of the observed NOEs.

A total of 32 transfer NOEs was observed for butirosin A in the APH(3′)-IIIa·ATP·butirosin A ternary complex. There were 17 intra-ring transfer NOEs that serve to define the conformation of the three rings. A total of 5 intra-chain NOEs were observed among the protons of the AHB chain. The remaining 10 transfer NOEs are inter-ring/chain and serve to define the conformational nature of enzyme-bound butirosin A. These NOEs are listed in Table 1, with the distance constraints derived from the data obtained in the 80 ms TRNOE experiment. A portion of this spectrum is presented in Figure 3A, which shows interglycosidic and long range NOEs.

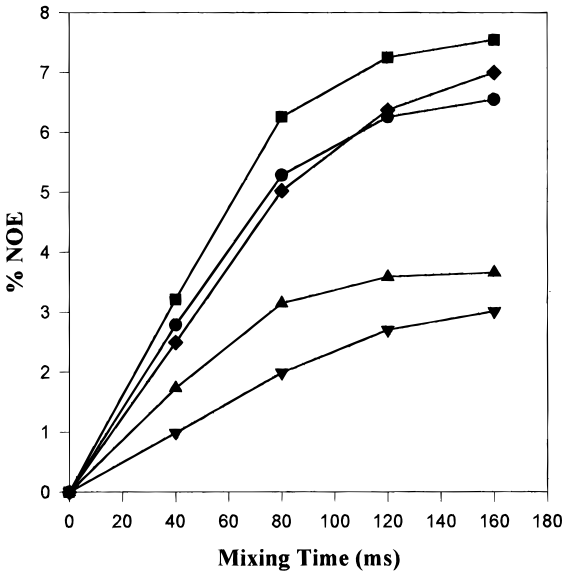

FIGURE 2: %NOE buildup curves for the following proton pairs: H3′−H5″ (■), H2e−H1 (◆), H1′−H4 (●), H1″−H2″ (▲), and H1′−H3 (▼). %NOE values were calculated by taking the ratio of the cross-peak volume of the NOE of interest to the volume of the H3‴−H3‴ cross-peak, at each mixing time.

Table 1: Inter-Ring/Chain Transfer NOEs for Butirosin A from the 80 ms TRNOESY Spectrum and the Calculated Distance Constraints[a]

NOE	lower limit (Å)[b]	upper limit (Å)
H1′−H3	3.2	3.7
H1′−H4	2.5	2.8
H1′−H5″[c]	4.1	4.5
H2′−H5″	3.8	4.4
H3′−H5″	2.3	2.6
H5′−H5″	3.4	3.9
H1″−H1	3.7	4.1
H1″−H5	2.2	2.5
H1″−H6	3.1	3.6
H2‴−H1	2.7	3.1

[a] The distances were calculated from the isolated spin pair approximation with the H1′−H2′ proton pair taken as the calibration distance (r = 2.38 Å). [b] A generous error of ±40% was used for the intensities of the NOEs in order to calculate the distance constraints. All constraints involving H5″ were assigned to the *pro-S* hydrogen.

TRNOESY Spectra of Amikacin. There were a total of 23 transfer NOEs observed for amikacin in the APH(3′)-IIIa·ATP·amikacin ternary complex. However, spectral overlap of important NOEs prevents a quantitative analysis. A portion of the 80 ms mixing time experiment is presented in Figure 3B. In this spectrum, the H1″−H5 and H1″−H6 NOEs are under the same cross-peak (g). Also, the H1′−H5 and H1′−H3′ NOEs appear under the same cross-peak (h) in the 80 ms experiment. The assignment of H5, H6, and H3′ in these two cross-peaks comes from the one-dimensional ^{1}H assignments of amikacin (Anderson *et al.*,

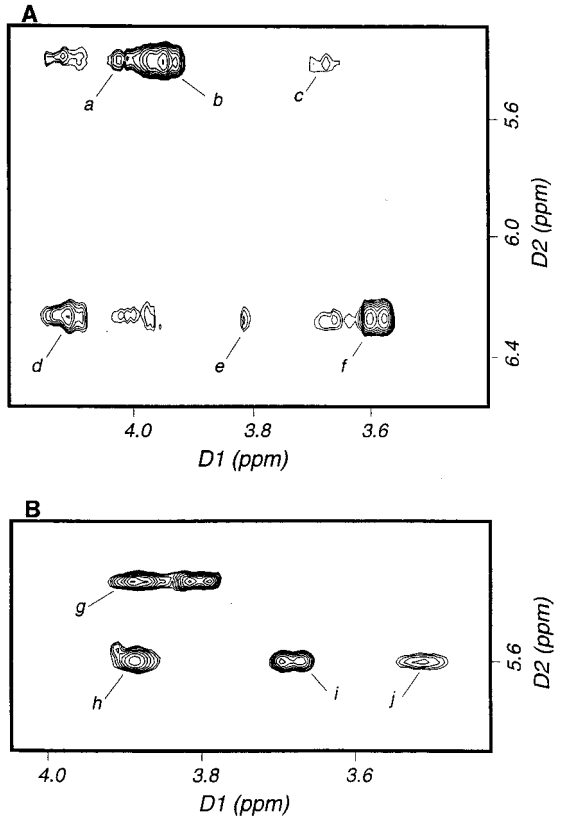

FIGURE 3: Regions of the TRNOE spectrum (80 ms) of butirosin A (A) and amikacin (B). The cross-peaks labeled in the butirosin A spectrum are H1″−H1 (a), H1″−H5 (b), H1″−H6 (c), H1′−H4 (d), H1′−H5″ (e), and H1′−H3 (f). The cross-peaks labeled in the amikacin spectrum are H1″−H5/H1″−H6 (g), H1′−H5/H1′−H3′ (h), H1′−H4 (i), and H1′−H3 (j). Cross-peaks not labeled in A and B represent intra-ring NOEs. The samples for the TRNOE spectroscopy contained 0.20 mM APH(3′)−IIIa, 5 mM antibiotic, 5 mM ATP, 5 mM $CaCl_2$, and 20 mM Tris-d_{11} buffer (pH 6.8).

Table 2: ^{15}N Assignments of Butirosin A at pH 5.90

nitrogen	chemical shift (δ, ppm)
N1	99.3
N3	16.6
N2′	11.3
N6′	4.02
N4‴	10.01

[a] All chemical shift values have been referenced to $^{15}NH_4Cl$ in 85:15 (v:v) H_2O/D_2O.

1988; Thompson *et al*., 1996a) and additional connectivities in the TRNOESY spectra.

pH Dependence of ^{15}N Chemical Shifts. The ^{15}N resonances for amikacin at pH 5.40 have been previously assigned (Schanck *et al*., 1992), and the ^{15}N assignments of butirosin A were made in this study at pH 1.0 where the ammonium protons were easily visible in the ^{1}H NMR spectrum of butirosin A. The ^{1}H-^{1}H COSY (spectrum not shown) experiment allowed the assignment of amine protons on the basis of connectivity with vicinal carbon-bound protons. The ^{1}H−^{15}N HSQC (spectrum not shown) experiment allowed the ^{15}N assignments on the basis of connectivity of the nitrogen-bound protons assigned in the COSY experiment. The ^{15}N assignments of butirosin A, at pH 5.90, are given in Table 2. The reporting of the chemical shifts at this pH allows a more direct comparison of the previously reported ^{15}N chemical shifts of amikacin (Schanck *et al*., 1992).

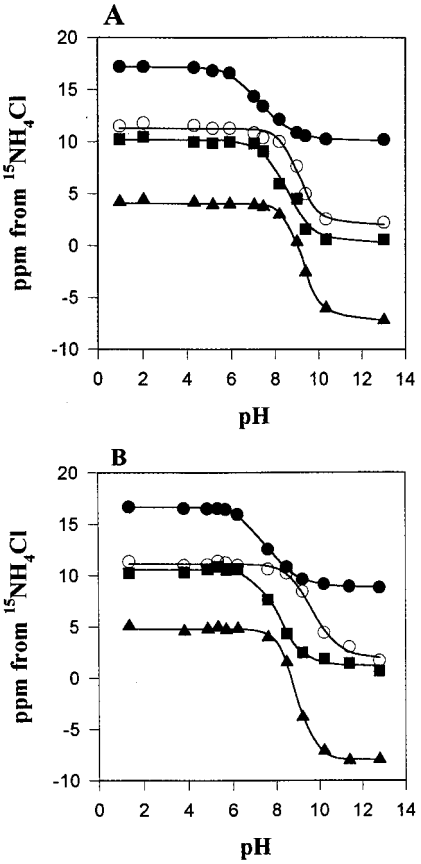

FIGURE 4: pH dependence of ^{15}N chemical shifts for butirosin A (A) and amikacin (B). The titration curves for the amino groups at N3 (●), N2′ (○), N4‴ (■), and N6′(▲) in butirosin A and at N3 (●), N3″ (○), N4‴ (■), and N6′ (▲) in amikacin are presented. The samples initially contained 0.5 M butirosin A or 0.8 M amikacin in 85:15 (v:v) H_2O/D_2O.

Table 3: pK_a Values[a] of the Amino Groups of and Amikacin and Butirosin A

	pK_a	
amino group nitrogen	amikacin	butirosin A
N3	7.62 ± 0.04	7.40 ± 0.05
N2′		9.11 ± 0.08
N6′	8.92 ± 0.03	9.37 ± 0.14
N3″	9.70 ± 0.09	
N4‴	8.13 ± 0.07	8.56 ± 0.04

[a]Midpoints of the titration curves of ^{15}N chemical shifts vs pH.

The complete pH dependence of the ^{15}N chemical shifts of butirosin A and amikacin is shown in panels A and B of Figure 4, respectively. The pK_as calculated from the titration curves are presented in Table 3. The amide proton at N1 in each antibiotic did not titrate over the pH values used in this study.

APH(3′)-IIIa-Bound Butirosin A. Eight of the final structures generated from the dynamics and minimization routines were superimposed at the 2-deoxystreptamine ring and appear in Figure 5. The glycosidic dihedral angles of butirosin A can be defined as Φ_1 (H1′−C1′−O_α−C4), Ψ_1 (H4−C4−O_α−C1′), Φ_2 (H1″−C1″−O_β−C5), and Ψ_2 (H5−C5−O_β−C1″). The average values of these dihedral angles for the eight butirosin A structures are as follows: $\Phi_1 = 11 \pm 6°$, $\Psi_1 = 49 \pm 3°$, $\Phi_2 = 13 \pm 18°$, and $\Psi_2 = 48 \pm 3°$. In panels A and B of Figure 6, the eight butirosin A structures are again superimposed; however, only the ring atoms, 3′

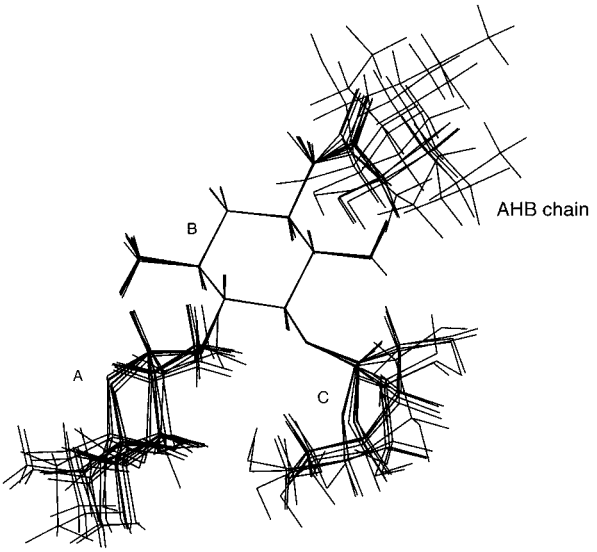

FIGURE 5: Representation of the APH(3′)-IIIa-bound conformations of butirosin A. These structures were obtained from energy minimization and dynamics routes with the distance constraints derived from the TRNOE experiments. The structures have been superimposed at the 2-deoxystreptamine ring (ring B). Each ring is labeled with its letter designation.

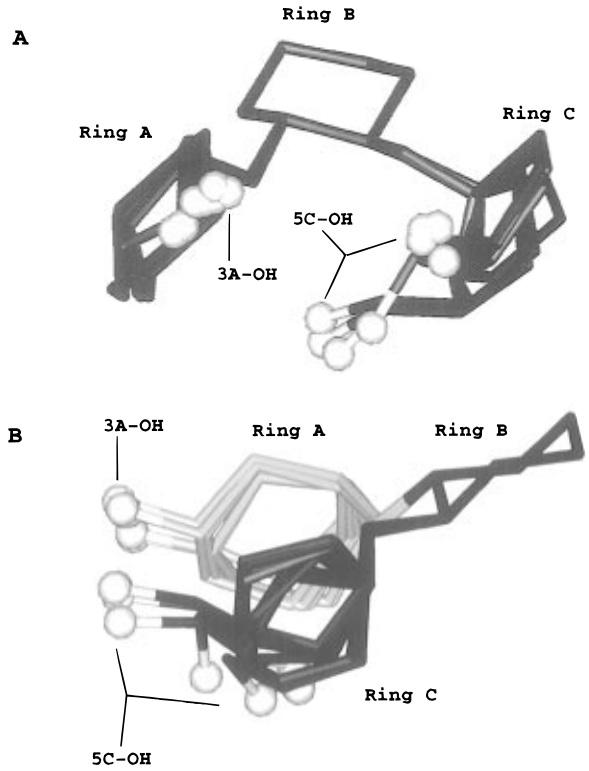

FIGURE 6: Superimposed structures of butirosin A with only the ring atoms and the 3′ (3A)- and 5″ (5C)-oxygens represented. Part A shows the the front view of the butirosin A structures, and part B shows a side view of the structures. The balls represent 3A- or 5C-oxygens.

(3A)-oxygens, and 5″ (5C)-oxygens are shown. The structures of butirosin A presented in Figures 5 and 6 do not violate the distance constraints (within the error limits) derived from the TRNOE studies.

DISCUSSION

Transferred nuclear Overhauser effect spectroscopy is one of the most powerful methods of determining the conformation of protein-bound ligands (Ni & Scheraga, 1994). For example, TRNOE methods have recently been used to determine bioactive conformations of sialyl-Lewis X (Scheffler *et al*., 1995; Cooke *et al*., 1994) and a blood group A trisaccharide (Casset *et al*., 1996).

The binding-induced NMR relaxation enhancements observed with transferred nuclear Overhauser effects require that the ligand under consideration be in fast exchange during complex formation (Ni, 1994). The relaxation enhancements can be observed at a high ligand:protein ratio where conformational information of bound ligands is transferred to the free ligands due to the binding event (Gronenborn & Clore, 1990). Previous studies with amikacin and butirosin A demonstrated that these antibiotics were appropriate for the TRNOE studies because they are in fast exchange from APH(3′)-IIIa·CrATP·antibiotic ternary complexes (Cox *et al*., 1996).

Studies with tobramycin (Dorman *et al*., 1976), a 4,6-disubstituted antibiotic, and neomycin B (Botto & Coxon, 1983), a 4,5-disubstituted antibiotic, revealed that both have one amino group with an unusually low pK_a value. Both of these aminoglycosides have amino groups at N1 and N3 of the 2-deoxystreptamine ring, and charge repulsion is believed to account for the low pK_a values of 6.2 (N1) for tobramycin and 5.7 (N3) for neomycin B. Therefore, it was necessary to determine the pK_a values for the amino groups of amikacin and butirosin A. As seen in Table 3, the amino groups at N3 of amikacin and butirosin A have lowered pK_a values, but not to the extent of those mentioned above for tobramycin and neomycin B. There have been no reports of pK_a values for the amino groups of aminoglycosides that have the 2-deoxystreptamine ring modified at N1 with the AHB chain. The partial positively charged amide nitrogen (N1) of the AHB chain may serve to slightly perturb the pK_a value of the amino group at N3 of amikacin and butirosin A, also through a charge repulsion phenomenon.

The importance of protonated amino (ammonium) groups to the phosphorylation of neamine and kanamycin A, catalyzed by APH(3′)-Ia and APH(3′)-IIa, has been demonstrated (Roestamadji *et al*., 1995). Removing one amino group significantly reduced the catalytic efficiencies of the enzymes by primarily reducing the turnover number (k_{cat}) of the antibiotic substrates. Moreover, similar studies with APH(3′)-IIIa have also demonstrated the importance of amino groups to the recognition of the enzyme by aminoglycoside substrates (McKay *et al*., 1996). These results, also based on kinetic studies, do not preclude the existence of ion-pairing interactions between the antibiotic molecules and residues present at the active site of APH(3′)-IIIa.

Another example of the importance of the charge state of aminoglycosides is the inhibition of the hammerhead ribozyme. The ionic interaction of the ammonium ions of neomycin B, with the hammerhead ribozyme, has been reported to mediate the inhibition (Clouet-d'Orval *et al*., 1995).

On the basis of the above observations, electrostatic interactions are likely important in the binding of aminoglycoside antibiotics to APH(3′)-IIIa. Additionally, there were no highly perturbed pK_a values for the amino groups of butirosin A or amikacin. Therefore, all of the amino groups of butirosin A were largely protonated at the pH in which the TRNOE studies were performed. As a result, the amino

groups were converted to ammonium ions in the minimization and dynamics routines described in this paper.

The widespread distribution of genes encoding aminoglycoside-phosphorylating enzymes has virtually eliminated the use of aminoglycoside antibiotics containing a 3′-OH group. The exception is amikacin, a semisynthetic aminoglycoside, which still finds some clinical utility. We have recently demonstrated that the arrangement of amikacin at the active site of APH(3′)-IIIa may account for the inefficient phosphorylation of amikacin due to difficulty in obtaining a productive collision in the ternary complex (Cox *et al.*, 1996).

In the TRNOESY spectrum presented in Figure 3B, there are three strong NOEs across the glycosidic linkage involving H1′. The NOEs H1′−H5, H1′−H4, and H1′−H3 are visible even in the shortest mixing time experiment (40 ms). The observed intensity of the overlapping H1′−H5 and H1′−H3′ cross-peak (h) indicates that a strong H1′−H5 NOE must contribute to the volume of this cross-peak. The H1′−H3′ contribution to this cross-peak should be minor due to the distance between these two protons in the chair conformation of the primed ring (ring A), as presented in Figure 6. Therefore, the H1′−H5 cross-peak should be the major contributor to the intensity of cross-peak h in Figure 3B. The observation of strong H1′−H3 and H1′−H5 NOEs, along with modeling studies, suggests that different enzyme-bound conformations of amikacin are present in ternary complexes in which there are significant differences in the glycosidic torsional angles around O_α, which links ring A and ring B.

One could argue that the enzyme binds amikacin in which ring A can have a variety of Φ and Ψ values. This would create a population of APH(3′)-IIIa·ATP·amikacin ternary complexes in which the 3′-OH of amikacin is in a reactive position and a population where the 3′-OH is not in the correct position to attack the γ-phosphate of ATP. Alternatively, ring A may be mobile while amikacin is bound to the active site of the enzyme. If ring A adopts a conformation where the 3′-OH can attack the γ-phosphoryl group of ATP, phosphorylation can occur and the modified antibiotic will be released. In some cases, ring A may not place the 3′-OH into a reactive position and the antibiotic will be released unmodified. Support for the above hypotheses may come from the fact that the phosphorylation of amikacin, catalyzed by APH(3′)-IIIa, is inefficient compared to other aminoglycoside antibiotics, and its K_m value is one order of magnitude higher than those of other substrates (McKay *et al*., 1994).

Intra-ring transfer NOEs observed between the protons of amikacin support the chair conformations of rings A−C presented in Figure 1. For example, the following strong transfer NOEs were observed in these rings: H3′−H5′, H3″−H5″, and H2ax−H6. All of the amino, hydroxyl, and hydroxymethyl groups in amikacin occupy equatorial positions, with the pyranose rings adopting a $^4C_1$ conformation.

The results from the paramagnetic NMR relaxation and TRNOE studies of amikacin provide insight into the interaction of this antibiotic with APH(3′)-IIIa. Amikacin is structurally unique among other substrates of the enzyme. It is 4,6-disubstituted at the 2-deoxystreptamine ring which is modified at N1 with the AHB chain. These unique structural features most likely dictate the geometry and dynamics of enzyme-bound amikacin. As a result, amikacin is poorly phosphorylated *in vivo* and is still a clinically useful antibiotic.

Previous paramagnetic NMR relaxation studies suggested that enzyme-bound butirosin A has the 2,6-diamino-2,6-dideoxy-D-glucose (ring A) and D-xylose (ring C) rings in a stacking arrangement (Cox *et al.*, 1996). This allows both the 3′- and 5″-OH groups to be extended out toward the γ-phosphoryl group of ATP in the ternary complex. The fact that there were four transfer NOEs between H5″ and ring A suggests that rings A and C are close to each other. In fact, the superimposed structures of butirosin A in Figures 5 and 6 also show that these two rings are in a stacking arrangement in enzyme-bound butirosin A. Figure 5 shows that the three rings of butirosin A have restricted motions when bound to the active site of APH(3′)-IIIa. On the other hand, the AHB chain can adopt a variety of conformations.

The distance constraints, derived from the 17 intra-ring NOEs and molecular modeling studies, show that rings A and B adopt chair conformations as presented in Figure 1, with the amino, hydroxyl, and hydroxymethyl groups occupying equatorial positions. As in amikacin, the pyranose ring (ring A) of butirosin A is rigid, with a $^4C_1$ conformation.

Panels A and B of Figure 6 focus on the relative positions of the 3′- and 5″-oxygens. In some structures, the 5″-oxygens are extended outward in the same plane as the 3′-oxygens. In the remaining structures, the 5″-oxygens are pointing in the opposite direction and not in an optimal position to be involved in a nucleophilic attack on the γ-phosphate of ATP. This may explain the observed preference for the initial phosphorylation event to occur at the 3′-OH of butirosin A. In fact, initial phosphorylation at this site occurs between 70 and 75% of the time, with the second phosphorylation reaction occurring at the 5″-OH (Thompson *et al*., 1996a).

The initial phosphorylation of butirosin A is much faster than the second phosphorylation reaction. This is not observed with ribostamycin and neomycin B, other 4,5-disubstituted aminoglycosides with 3′- and 5″-OH groups, because both the phosphorylation reactions occur at approximately equal rates. The fact that these other aminoglycosides do not have the AHB tail and the fact that they are easily diphosphorylated point to an important role of the AHB tail in the recognition of phosphorylated butirosin A by APH(3′)-IIIa.

It is intriguing that monophosphorylated butirosin A can bind to APH(3′)-IIIa and put the 3′- or 5″-OH into a reactive position. One plausible explanation is that the negatively charged phosphoryl group of monophosphorylated butirosin A is directed toward the positively charged Mg^{2+} ion of MgATP. This would prevent the 3′- or 5″-phosphoryl group from directly approaching the γ-phosphoryl group of ATP and avoid steric and electronic repulsion. A model can be built where the 3′-phosphoryl group of butirosin A coordinates Mg^{2+} and the 5″-OH is colinear and approximately 4 Å from the γ-phosphate of ATP. This model conserves the stacking of rings A and C, which seems to persist in solution (Cox & Serpersu, 1995) and at the active site of the enzyme, but overall requires a different arrangement of the antibiotic with respect to the triphosphate moiety of ATP. This is not unreasonable because APH(3′)-IIIa phosphorylates a broad range of substrates with different ring architectures. Additionally, the coordination of the phosphoryl group of 3-phospho-D-glycerate, to the metal ion of a MeATP

complex, has been shown to occur in the phosphorylation reaction catalyzed by phosphoglycerate kinase (PGK), to produce 1,3-bisphosphoglycerate (Pappu *et al*., 1994). Conformational studies with 3′-phosphorylated butirosin A, both in solution and bound to APH(3′)-IIIa, are a logical extension of the work presented in this report.

Transferred nuclear Overhauser effect spectroscopy and molecular modeling were used to gain insight into the geometry and dynamics of APH(3′)-IIIa-bound aminoglycoside antibiotics. The results presented here provide insight into how APH(3′)-IIIa interacts with amikacin and butirosin A and serve to explain the regiochemistry of phosphorylation observed with butirosin A. This work will also complement X-ray diffraction studies, which are currently in progress (G. Wright, personal communication). In addition, the enzyme-bound conformation of butirosin A can be utilized as a template in a computer-aided drug design program, which is also in progress in this laboratory. Programs such as CAVEAT (Lauri & Bartlett, 1994) can use the geometrical characteristics of known ligands to design inhibitors of biological targets such as enzymes of therapeutic interest.

ACKNOWLEDGMENT

We thank Dr. David Baker for his gift of butirosin A and Geoffrey McKay and Dr. Gerard Wright, of McMaster University, for the critical reading of the manuscript. We acknowledge Bob Johnson and the Division of Biology Computer Imaging Research Facility for help in preparing Figure 6.

REFERENCES

Anderson, N. H., Eaton, H. L., Nguyen, K. T., Hartzell, C., Nelson, R. J., & Priest, J. H. (1988) *Biochemistry 27*, 2782−2790.

Botto, R. E., & Coxon, B. (1983) *J. Am. Chem. Soc. 105*, 1021−1028.

Casset, F., Peters, T., Etzler, M., Korchagina, E., Nifant'ev, N., Pérez, S., & Imberty, A. (1996) *Eur. J. Biochem. 239*, 710−719.

Clouet-d'Orval, B., Stage, T. K., & Uhlenbeck, O. C. (1995) *Biochemistry 34*, 11186−11190.

Cooke, R. M., Hale, R. S., Lister, S. G., Shah, G., & Weir, M. P. (1994) *Biochemistry 33*, 10591−10596.

Cox, J. R., & Serpersu, E. H. (1995) *Carbohydr. Res. 271*, 55−63.

Cox, J. R., McKay, G. A., Wright, G. D., & Serpersu, E. H. (1996) *J. Am. Chem. Soc. 118*, 1295−1301.

Davies, J. (1994) *Science 264*, 375−381.

Davis, B. D. (1987) *Microbiol. Rev. 51*, 341−350.

Dorman, D. E., Paschal, J. W., & Merkel, K. E. (1976) *J. Am. Chem. Soc. 98*, 6885−6888.

Gronenborn, A. M., & Clore, G. M. (1985) *Prog. Nucl. Magn. Reson. Spectrosc. 17*, 1−32.

Gronenborn, A. M., & Clore, G. M. (1990) *Biochem. Pharmacol. 40*, 115−119.

Homans, S. W. (1990) *Biochemistry 29*, 9110−9118.

Marion, D., & Wutrich, K. (1983) *Biochem. Biophys. Res. Commun. 113*, 967−974.

Markley, J. L. (1975) *Acc. Chem. Res. 8*, 70−80.

McKay, G. A., & Wright, G. D. (1995) *J. Biol. Chem. 270*, 24686−24692.

McKay, G. A., & Wright, G. D. (1996) *Biochemistry 35*, 8680−8685.

McKay, G. A., Thompson, P. R., & Wright, G. D. (1994) *Biochemistry 33*, 6936−6944.

McKay, G. A., Roestamadji, J., Mobashery, S., & Wright, G. D. (1996) *Antimicrob. Agents Chemother. 40*, 2648−2650.

Ni, F. (1994) *Prog. Nucl. Magn. Reson. Spectrosc. 26*, 517−606.

Ni, F., & Scheraga, H. A. (1994) *Acc. Chem. Res. 27*, 257−264.

Pappu, K. M., Gregory, J. D., & Serpersu, E. H. (1994) *Arch. Biochem. Biophys. 311*, 503−508.

Roestamadji, J., Grapsas, I., & Mobashery, S. (1995) *J. Am. Chem. Soc. 117*, 11060−11069.

Schanck, A., Brasseur, R., Mingeot-Leclercq, M.-P., & Tulkens, P. M. (1992) *Magn. Reson. Chem. 30*, 11−15.

Schatz, A., Bugie, E., & Waksman, S. A. (1944) *Proc. Soc. Exp. Biol. Med. 55*, 66−69.

Scheffler, K., Ernst, B., Katopodis, A., Magnani, J. L., Wang, W. T., Weisemann, R., & Peters, T. (1995) *Angew. Chem., Int. Ed. Engl. 34*, 1841−1844.

Shaw, K. J., Rather, P. N., Hare, R. S., & Miller, G. H. (1993) *Microbiol. Rev. 57*, 138−163.

Thompson, P. R., Hughes, D. W., & Wright, G. D. (1996a) *Biochemistry 35*, 8686−8695.

Thompson, P. R., Hughes, D. W., & Wright, G. D. (1996b) *Chem. Biol. 3*, 747−755.

Umezawa, H., & Kondo, S. (1982) in *Aminoglycoside Antibiotics* (Umezawa, H., & Hooper, I. R., Eds.) pp 267−292, Springer-Verlag, Berlin.

Weiner, S. J., Kollman, P. A., Nguyen, D. T., & Case, D. A. (1986) *J. Comput. Chem. 7*, 230−252.

BI9626822